RESEARCH

Effects of fuel and driving conditions on particle number emissions of China-VI gasoline vehicles: based on corrections to test results

Xiaohan Miao · Xin Zhang · Chang Wang · Jingyuan Li · Jie Zhao · Liang Qu · Yu Liu · Songbo Qi · Honglin Li · Mengqi Fu · Taosheng Jin

Abstract The increasing number of vehicles are emitting a large amount of particles into the atmosphere, causing serious harm to the ecological environment and human health. This study conducted the Worldwide Harmonized Light Vehicles Test Cycle (WLTC) to investigate the emission characteristics of particle number (PN) of China-VI gasoline vehicles with different gasoline. The gasoline with lower aromatic hydrocarbons and olefins reduced particulate matter (PM) and PN emissions by 24% and 52% respectively. The average PN emission rate of the four vehicles during the first 300 s (the cold start period) was 7.2 times that of the 300 s–1800s. Additionally, because the particle transmission time and instrument response time, the test results of instantaneous emissions of PN were not synchronized with vehicle specific power (VSP). By calculating the Spearman correlation coefficient between pre-average vehicle specific power (PAVSP) and the test results of PN instantaneous emissions, the delay time was determined as 10s. After the PN emissions results were corrected, the PN emissions were found to be more related to VSP. By analyzing the influence of driving status on emission, this study found that vehicles in acceleration mode increased PN emissions by 76% compared to those in constant speed mode.

X. Miao · C. Wang · L. Qu · T. Jin (✉)
Tianjin Key Laboratory of Urban Transport Emission Research, College of Environmental Science and Engineering, Nankai University, Tianjin 300350, China
e-mail: jints@nankai.edu.cn

X. Zhang · J. Li (✉) · Yu. Liu · S. Qi · H. Li
China Automotive Technology and Research Center Co., Ltd., Tianjin 300300, China
e-mail: lijingyuan@catarc.ac.cn

J. Zhao
Research Institute of Petroleum Processing, SINOPEC, Beijing 100083, China

M. Fu
School of Environmental Science and Safety Engineering, Tianjin University of Technology, Tianjin 300384, China

Introduction

China has become the world's largest vehicle sales country (Liu et al., 2020). A large number of vehicles directly emitted significant amounts of greenhouse gases and particulate matter (PM) into the atmosphere, with PM emissions reaching 69,000 tons in 2021 (MEE, 2022). Particles scatter and absorb sunlight, decreasing visibility and having an impact on

global climate change (Yang et al., 2021). Fine particles stay longer in the atmosphere and had a greater impact than coarse particulate matter (Fang et al., 2021; Ioannis et al., 2020). Exposure to high concentrations of particle is harmful to human health. Previous research has identified $PM_{2.5}$ as the world's fifth leading cause of death (Hannelore et al., 2019; Wu et al., 2018). $PM_{2.5}$ in the outdoor environment of China causes more than 1 million premature deaths and more than 20 million life losses each year (Abhishek & Orathai, 2023; Li et al., 2016). The World Health Organization advises that the annual mean concentration of $PM_{2.5}$ in the atmosphere be kept below 5 μg/m^3, which could reduce deaths from exposure to $PM_{2.5}$ by more than 80% (WHO, 2021).

Particle emissions from vehicles are affected by a variety of parameters, including vehicle type (model and degree of deterioration), fuel properties and combustion, driving conditions, engine load, environment, and coolant temperature (Xu et al., 2020). Particle emissions are mostly caused by incomplete combustion (Banerjee & Christian, 2017), and fuel characteristics are directly related to combustion, which influences exhaust emissions. Researchers have found that fuel with lower aromatics content can significantly reduce the emission of particle and other pollutants(Pan et al., 2019; Zhang et al., 2022). In addition, particle number (PN) emissions increase in intense driving situations. For example, Gallus et al. found that PN emissions increased with higher acceleration, which was associated with high engine loads (Gallus et al., 2016). Vehicles generated a large amount of particulate matter during the cold start process. According to Chen et al. (Chen et al., 2017), under the New European Driving Cycle (NEDC), Gasoline Direct Injection (GDI) vehicles emitted PN during cold starts, accounting for over 50% of the entire NEDC, while Port Fuel Injection (PFI) vehicles emitted more than 70% during cold starts.

Vehicle specific power (VSP) was closely related to vehicle pollutant emissions, for example, the MOVES model used VSP to describe the driving behavior and emission status of different types of vehicles (An et al., 1997; EPA, 2009; Lents & Davis, 2004; Liu & Barth, 2012). However, the transmission time of the particles in the test system and instrument response time generated some delay time between the true value and the measured value of instantaneous PN emissions. The presence of delay time causes the VSP of the vehicle and the emission test results to be out of synchronization, affecting the vehicle's emission level evaluation under transient conditions. The IVE model uses the pre-average vehicle specific power (PAVSP) of the average VSP in the 0–15 s before the current second(Davis et al., 2005) and the PAVSP is more correlated with the uncorrected instantaneous emission results.

This study utilized gasoline vehicles compliant with the China VI emission standard, which was the strictest emission standard in China at the time. The gasoline used adhered to the Beijing VI A or Beijing VI B gasoline standard, and the latter was the strictest gasoline standard for vehicles in China. This standard had been enforced in Beijing, China, and was in use throughout the year. In this study, based on bench experiments, the second-by-second PN emissions of China-VI vehicles with two different gasoline fuels were tested on a chassis dynamometer. PN emissions of China VI vehicles under different driving conditions were evaluated, and the further reduction in particulate emissions brought about by the upgrade in gasoline was analyzed. The most likely delay time was identified by calculating the Spearman correlation coefficient between PAVSP at different average times and test results of PN instantaneous emission, resolving the problem that instantaneous PN emissions were not synced with VSP. To investigate the association between PN emissions and driving status, the corrected test results of PN instantaneous emissions were used.

Materials and methods

Test fuels

This study utilized gas chromatography to determine the alkane, cycloalkane, olefin, aromatic, and oxygenated compound compositions of two types of gasoline, and analyzed their physical properties. The specific characteristics of the two gasoline fuels were shown in Table 1. Compared to gasoline A, gasoline B had lower aromatic hydrocarbons and olefin content.

Test vehicles

Four light passenger vehicles that met the China-VI emission standard (MEE, 2016) were used, with

Table 1 The main indexes of test gasoline

Gasoline	A	B
Research octane number	96.2	96.4
Density(20 °C)，kg/m^3	741.0	740.8
10% evaporation temperature(T10)，°C	65.0	59.0
50% evaporation temperature(T50)，°C	101.2	100.0
90% evaporation temperature(T90)，°C	186.8	165.9
Content of oxygen,%(mass fraction)	1.60	1.96
Content of aromatic hydrocarbons，%(volume fraction)	30.56	25.20
Content of olefin，%(volume fraction)	11.35	8.09

vehicles 1, 2, and 3 being GDI and vehicle 4 being a PFI. Details of each vehicle were shown in Table 2. Before each test, the test vehicles were placed in a test cell of 23 °C ± 2 °C. The engine oil and coolant reach a temperature of 23 °C ± 2 °C after 12 hours of soaking.

Test equipment and test cycle

The experiment was based on the full flow emission test system, which complied with the China-VI emission standard (MEE, 2016). The particle size range of the detected particles was greater than 23 nm. After sampling, the CVS dilution system diluted the exhaust, and PN was carried out using the AVL489 particle counter. One or more dilutions were performed on the sample gas to bring the particle number concentration below the upper limit of detection for the particle counter and the inlet temperature of the particle counter below 35 °C. The test cycle was the World Harmonized Light-duty vehicles Test

Cycle (WLTC) with cold start. With a total period of 1800 seconds and a top speed of 131.3 km/h, WLTC had four stages: low speed, medium speed, high speed, and ultra-high speed. Figure 1 depicts the distribution of driving time and speed.

Data analysis

*Test and calculation of PN and PM emission rates*

The test and calculation of PN and PM referred to (MEE, 2016). Exhaust gases were discharged from the vehicle's exhaust pipe, diluted, and then entered the sampling system, where they were counted after volatile particles were removed. The testing system automatically monitored the dilution factor of the exhaust gases. During the testing process, in order to minimize the impact of temperature changes caused by the mixing of exhaust and dilution gases, a heat exchanger was used to maintain the temperature within a certain range. During the PM sampling process, the sampling flow rate was proportional to the total dilution flow rate in the dilution channel, with a control error of less than 5%. PM was collected on filter paper and weighed. The instantaneous average values of PN emissions from the three experiments were taken as the experimental results, with PM treated similarly. The calculation method for PN emission rate is illustrated in eqs. 1–3.

Each experimental step in this study was strictly conducted according to detailed standard operating procedures, including experimental methods, instrument settings, data acquisition, and processing processes, ensuring the consistency of the experiments.

Table 2 The main parameters of four vehicles

Vehicle	Vehicle 1	Vehicle 2	Vehicle 3	Vehicle 4
emission standard	China-VI	China-VI	China-VI	China-VI
Running mass (kg)	1530	1722	1270	1240
Displacement (L)	1.5	2.0	1.4	1.5
Maximum net torque (Nm)	243	350	242	144
Aspiration	Turbocharged	Turbocharged	Turbocharged	Natural
Fuel Injection	GDI	GDI	GDI	PFI
Compression ratio	10.3	10.3	10	11
No. of Cylinders	4	4	4	4
Maximum speed(km/h)	190	230	190	190
After-Treatment	TWC + GPF	TWC + GPF	TWC + GPF	TWC + GPF
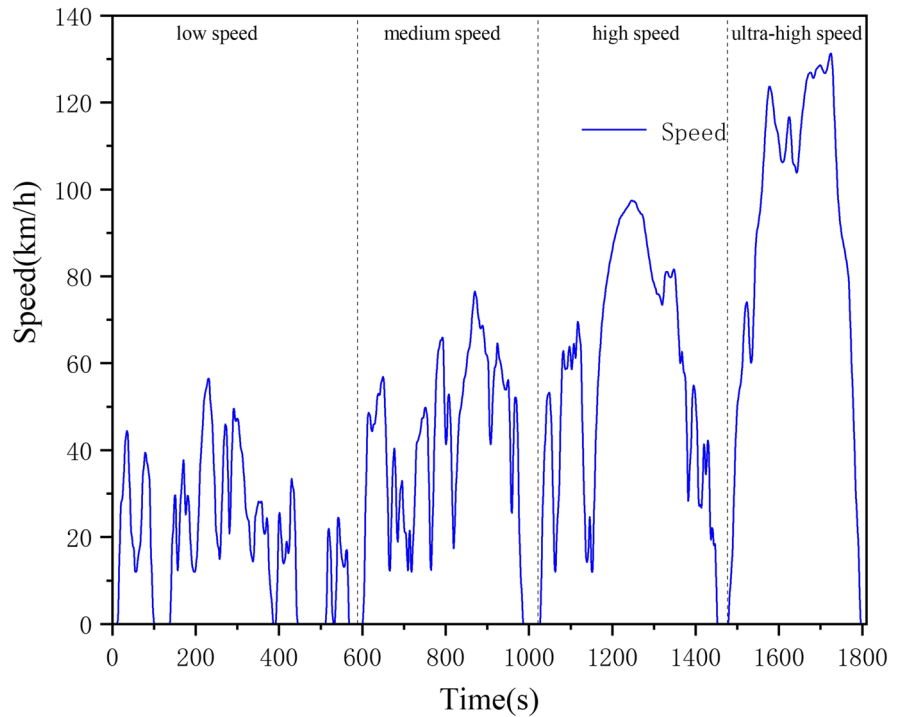
Instruments and equipment used were calibrated before and after experiments to ensure their accuracy and reliability. Replicate experiments were conducted to validate the consistency of the results. More than three replicate experiments were performed to ensure the repeatability of the experimental results, rather than being influenced by chance factors.

$$PN = \frac{V \times k \times \left(\overline{C_s} \times \overline{f_r} - C_b \times \overline{f_{rb}} \right) \times 10^3}{d} \quad (1)$$

Where PN denotes the particle number emission rate (#/km); V denotes the volume of the diluted exhaust (L); which is corrected to the standard state (273.15K, 101.325kPa); k denotes the correction factor, which is 1 here; $\overline{C_s}$ denotes the concentration of diluted exhaust particles in the standard state after correction (#/cm^3); C_b denotes the concentration of particulate number in the background of diluted air or diluted channel in the standard state (#/cm^3), measured before the experiment commenced; $\overline{f_r}$ denotes the average particle concentration reduction coefficient of the volatile particle remover set by dilution and particle loss during the test; $\overline{f_{rb}}$ denotes the average particle concentration reduction coefficient of the volatile particle remover set by dilution and particle

loss during the test; and *d* denotes the mileage of the test cycle (km).

$$PN_i = \frac{V \times k \times \left(\overline{C_{S,i}} \times \overline{f_r} - C_b \times \overline{f_{rb}} \right) \times 10^3}{t} \quad (2)$$

Where PN_i denotes the particle number instantaneous emission rate at i moment (#/s). $\overline{C_{S,i}}$ denotes the concentration of diluted exhaust particles in the standard state after correction at i moment(#/cm^3). And t was 1 s here.

$$PM = \frac{V_{mix} \times P_e}{V_{ep} \times d} \quad (3)$$

Where V_{mix} denotes the diluted exhaust volume in standard condition (m^3), V_{ep} denotes the exhaust volume of particulate matter filter membrane in the standard state (m^3), P_e denotes the weight of the particulate matter collected by filter membrane (mg), and d denotes the actual distance of the test cycle (km).

Acceleration

Acceleration was a parameter used to describe the speed change of the vehicle, the driving state of the

vehicle was divided into idle, uniform speed, acceleration, and deceleration of a total of four states.

According to the limits and measurement methods for emissions from light-duty vehicles (China-VI), the acceleration of the vehicle was calculated as shown in Eq. (4), and the acceleration was calculated sequentially for the instantaneous velocity measured second by second in the WLTC test cycle.

$$a_i = \frac{v_{i+1} - v_i}{3.6 \times (t_{i+1} - t_i)} \tag{4}$$

Where a_i denotes the acceleration of the test vehicle from moment i to moment i-1 (m/s^2), v_i denotes the speed of the test vehicle at moment t_i(km/h), and t_i denotes the time at moment i (s).

According to the difference in acceleration and speed, the driving state of the vehicle was divided into constant speed, acceleration, deceleration, and idle speed. The definition of driving state was shown in Table S1 of supporting information.

Vehicle specific power

Vehicle specific power (VSP) was the ratio of engine instantaneous output power to vehicle mass, kW/t. It was defined as the engine power needed to overcome the resistance between the vehicle and the surface of the road and the air when the vehicle was moving. It was a function of speed, acceleration, and road slope while the vehicle was driving, and its simplified equation was shown in Eq. (5) (Jiménez, 1999).

$$VSP = v \times (1.1 \times a + 9.81 \times (a \times \tan(\sin\theta_R)) + 0.132) + 0.000302 \times v^3 \tag{5}$$

Where v denotes the speed of vehicle (m/s), a denotes the acceleration (m/s^2), and θ_R denotes the road gradient. Since the test road was flat, θ_R was taken as 0 here.

To analyze the relationship between VSP and instantaneous PN emissions rates, an interval clustering analysis was performed on VSP. According to the study by Frey et al. (Frey et al., 2007). VSP values were divided into equally spaced bins with a minimum step size of 2 kW/t, and the average instantaneous emission rate for each bin was calculated. The first interval was defined as below −10 kW/t. Between −10 kW/t and 20 kW/t, there were 16 bins,

and VSP = 0 included a significant number of operating points, indicating idle vehicle status. Therefore, it was partitioned as a separate bin, and the final interval was for values greater than 20 kW/t, with specific divisions shown in Table 3.

Pre-average vehicle specific power and correction

Due to particle transport and instrument response time in the test system (MEE, 2016), the test results had a delay time with the true instantaneous emission level and were not synchronized with VSP. To reduce the impact of systematic errors, take the VSP average of 5 s,6 s,7 s,8 s,9 s,10s,11 s,12 s,13 s,14 s, and 15 s before the testing point as pre-average VSP, respectively (Zhou et al., 2019). And calculated the Spearman correlation coefficient ρ between VSP or PAVSP and the instantaneous emission rate of PN. The time corresponding to PAVSP with the highest correlation coefficient was taken as the correction time, and the instantaneous emission data of PN were advanced to take the real instantaneous emission level.

Results and discussion

Effect of different gasoline on PM and PN emissions

As indicated in Fig. 2, when using gasoline B instead of gasoline A, the PM emissions (Fig. 2a) of all test vehicles were reduced by an average of 24% ± 10% (the mean ± standard deviation), and the PN emissions (Fig. 2b) were reduced by an average of 52% ± 24%. The reduced aromatic hydrocarbon and

Table 3 Division of VSP bins

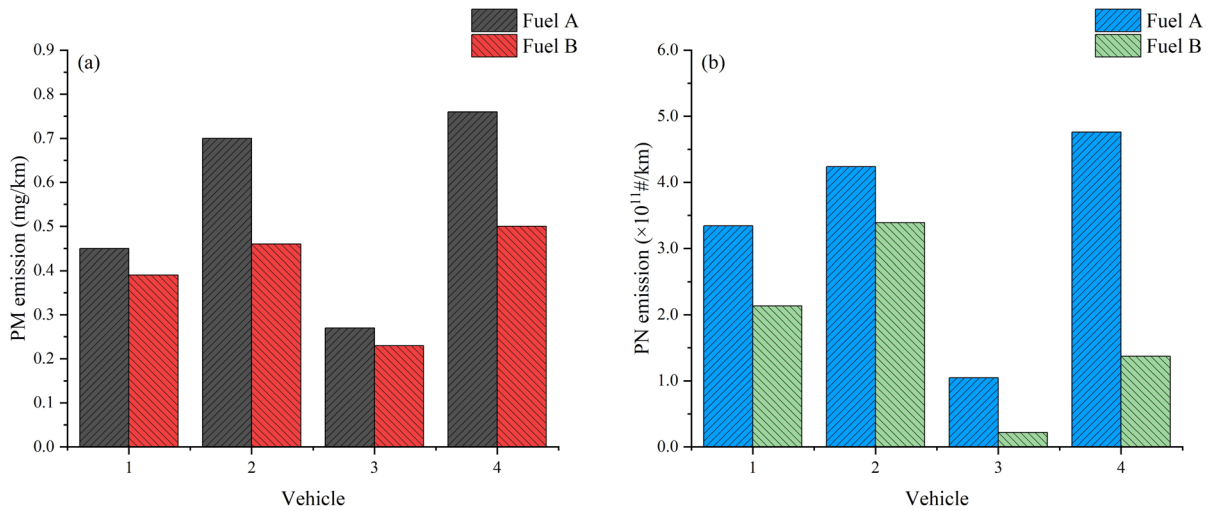| bin	VSP	bin	VSP
1	VSP < −10	10	4 ≤ VSP < 6
2	-10 ≤ VSP < −8	11	6 ≤ VSP < 8
3	-8 ≤ VSP < −6	12	8 ≤ VSP < 10
4	-6 ≤ VSP < −4	13	10 ≤ VSP < 12
5	-4 ≤ VSP < −2	14	12 ≤ VSP < 14
6	-2 ≤ VSP < 0	15	14 ≤ VSP < 16
7	VSP = 0	16	16 ≤ VSP < 18
8	0 < VSP < 2	17	18 ≤ VSP < 20
9	2 ≤ VSP < 4	18	VSP ≥ 20

Fig. 2 PM (**a**) and PN (**b**) emissions of each vehicle

olefin content of gasoline B was ascribed to the lower particle emissions. Georgios et al. evaluated the emissions of gasoline with aromatic hydrocarbon content of 15%, 25%, and 35%, respectively, and found that as compared to the former, the latter two had 148% and 330% higher PM levels (Karavalakis et al., 2015). Studies had shown that an increase in the aromatic hydrocarbon content in gasoline could exacerbate PM emissions (Yang et al., 2019). Because aromatic hydrocarbons possessed a stable benzene ring structure, a high molecular weight, and were difficult to completely combust, they were prone to particle formation.

Furthermore, the decline in olefin content was a significant factor in the decline of PM and PN. Wei et al. compared with the emissions of gasoline with olefin content of 8.2% and 17.2%, the PM and PN emissions of gasoline with a lower olefin content were significantly reduced, reaching 87.4% and 95.8% respectively(Wei et al., 2019). Wang et al. reported that using gasoline with a lower olefin content reduced PN emissions(Wang et al., 2016). Zhao et al. found that olefins in gasoline promoted the formation of aromatics and increased PN emissions(Zhao et al., 2017). Table S2 compared the fuel and results of this study to those of other researches. Furthermore, lowering T90 or T95, which represented 90% or 95% of the distillation temperature of gasoline, played an important impact in reducing PM and PN emissions. (Zhang et al., 2022).

The impact of cold start on emissions

Figure 3 showed instantaneous PN emissions of vehicle 1 during the WLTC test, while the instantaneous PN emissions of other vehicles were shown in Fig. S1 of the supporting information. Vehicles emitted a large amount of PN in the first 300 seconds. During the WLTC testing period, due to cold starts, the PN emissions from the first 300 seconds accounted for over 59% of the total PN emissions for all four vehicles. When using gasoline A, the average PN emission rate within the first 300 seconds was 1.74E+12 #/s for all four vehicles, while the average PN emission rate for the entire WLTC cycle was 4.07E+11 #/s. The average PN emissions rate of the four vehicles during the first 300 s was 7.2 ± 3.3 times that of the 300 s–1800s. PN emissions decreased quickly after the warm-up process. Other studies had discovered similar phenomena (Chen et al., 2017; Ko et al., 2019; Tang et al., 2022). Chen et al. found that the cold start emissions from the ECE 15 (urban driving cycle) within NEDC accounted for more than 50% of the total PN for GDIs and 70% for PFIs (Chen et al., 2017). The temperature inside the engine cylinder and exhaust components was low during the cold start, and speedy warm-up was achieved by increasing the fuel mixture (Alashaab et al., 2016). Low cylinder and coolant temperatures slowed down fuel evaporation, and insufficiently burned hydrocarbons and organic molecules were adsorbed and condensed

Fig. 3 Instantaneous PN emissions of vehicle 1
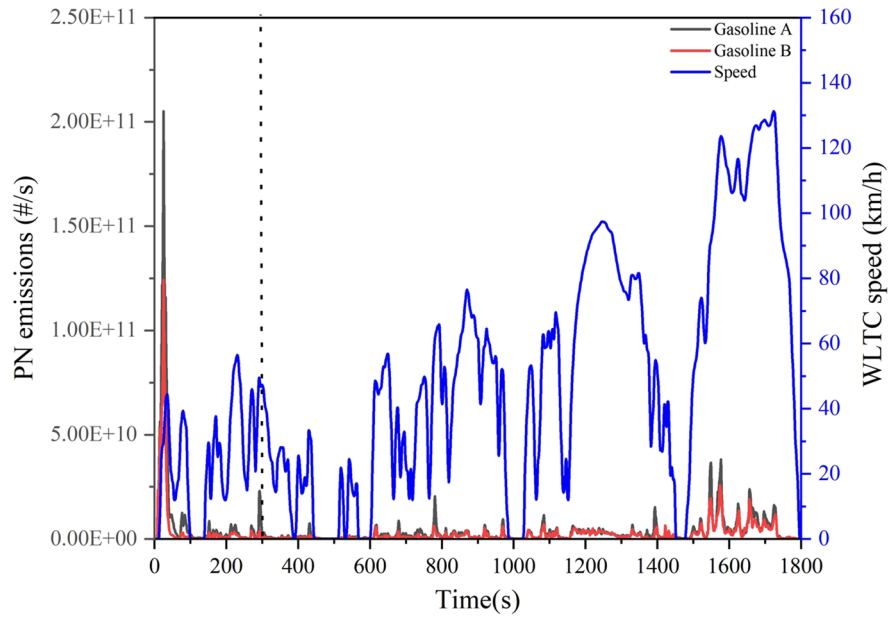
into a large amount of particulate matter in a short period of time (Liu et al., 2017).

Determination of the delay time and correction of the test results

Determination of the delay time

This study used the 300 s–1800s WLTC period to investigate the association between driving status and the results of PN emissions for each vehicle(Giechaskiel et al., 2019). The comparison of Spearman correlation coefficients ρ between VSP and each PAVSP was shown in Fig. 4. The correlation coefficient between PAVSP and the instantaneous emission rate of PN was much higher than that between VSP. Among each PAVSP, the correlation coefficient ρ between PAVSP-10s and PN instantaneous emission rate was the highest. The average value of ρ (PAVSP-10s) for three GDI vehicles (vehicle 1, 2 and 3) using two gasoline was 0.816, while for PFI vehicle (vehicle 4) was 0.522. The instantaneous emission rate of PN of the PFI vehicle was poorly correlated with VSP. Chen et al. found that the emission of PFI vehicles was more related to the engine torque while the correlation with speed and acceleration was negligible (Chen et al., 2017). Since there was only one PFI vehicle in this study, PAVSP also had a greater correlation coefficient with the instantaneous PN emissions rate of the PFI vehicle. Figure 5 presented the

correlation coefficient between the instantaneous PN emission concentration and VSP Spearman for Vehicle 1 when calibrated at different delay times using gasoline A. From Fig. 5, it was evident that the correlation between the instantaneous PN emission concentration and VSP was strongest when calibrated with a delay time of 10 seconds, indicating that 10 seconds was an appropriate delay time. As the calibration time continued to increase, the correlation decreased rapidly.

Due to the transmission time of particles in the test system and the response time of the instrument, there was some delay time between the true value and the measured value of instantaneous PN emission. This phenomenon caused PN test results were not synchronized with the vehicle's instantaneous driving behavior. Sandhu et al. reported errors on vehicle emission rates from Portable Emissions Measurement Systems, and modified the temporal gap between concurrent features until the features occurred at the same time (Sandhu & Frey, 2013). The delay time of 10s was proposed in this study and used to correct the PN emissions test result, which meant that the PN emissions result was advanced by 10s as the true value of the current working point.

Comparison before and after correction of PN emissions

The average PN emission rate for each bin was calculated based on the corrected results of four
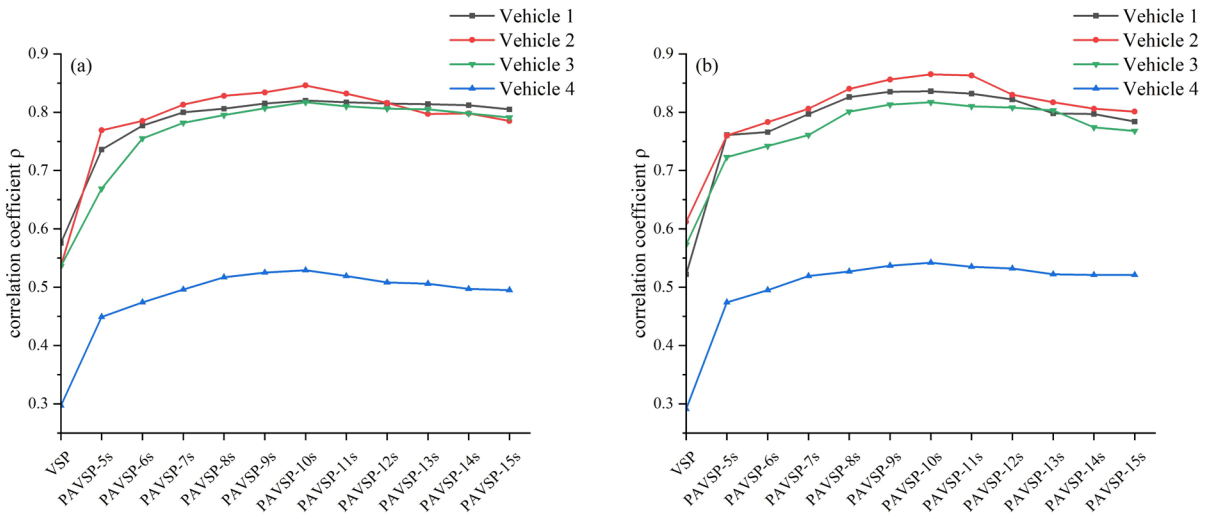
Fig. 4 Spearman correlation coefficients between VSP and each PAVSP of each vehicle with gasoline A (**a**) and gasoline B (**b**)
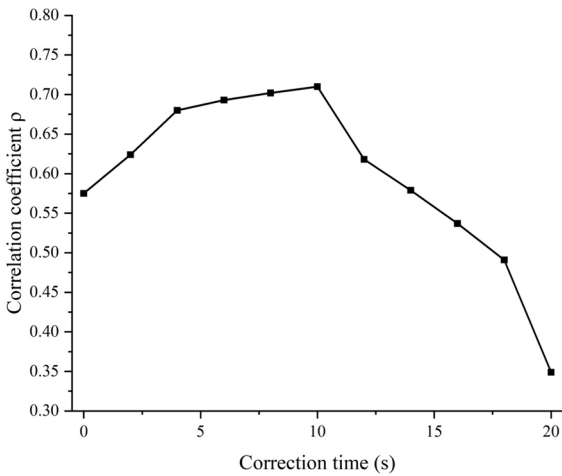

Fig. 5 The correlation coefficient between the instantaneous PN emission rate and VSP Spearman for Vehicle 1 at different correction times

vehicles. Figure 6 showed the PN emissions results of vehicle 1 with gasoline A before and after corrected in different VSP bins. Other situations were shown in Fig. S2. PN emissions in bins 1–6 (VSP < 0) fluctuated at a lower level. And the vehicle was idle during bin 7 (VSP = 0) and released the least PN emissions. Bins 8–18 showed an increasing trend in PN emissions. It was worth noting that the instantaneous VSP and PN emissions

were out-of-sync, which deviated from the emission calculation of each Bin, reducing the variability of emission rate with VSP, and averaged the emission results of each Bin. After correction the ratio of Bin's greatest to lowest average emission rates was 50.2. And it was 33.9 before correction. This was similar to the research phenomenon of Sandhu et al. They found that a 10s delay changed the ratio of the high modal average to the lowest modal to change from 80 to 22, This may also be related to the PEMS system they used (Sandhu & Frey, 2013).

The distribution of PN emissions before and after the correction with VSP of vehicle 1 was shown in Fig. 7. The coefficient (R^2) before the correction was between 0.33~0.41 and the coefficient after the correction was between 0.57~0.62 by fitting the third-order polynomial function. Before correction, the PN emissions were dispersed, and the law of change with VSP was not obvious. After correction, the PN distribution was more concentrated, and the trend with the growth of VSP was stronger, indicating that the synchronization of PN emissions and VSP was better after error correction.

Impact of driving behavior on emissions

According to the analysis results above, 10s was taken as the correction time, and the test result of

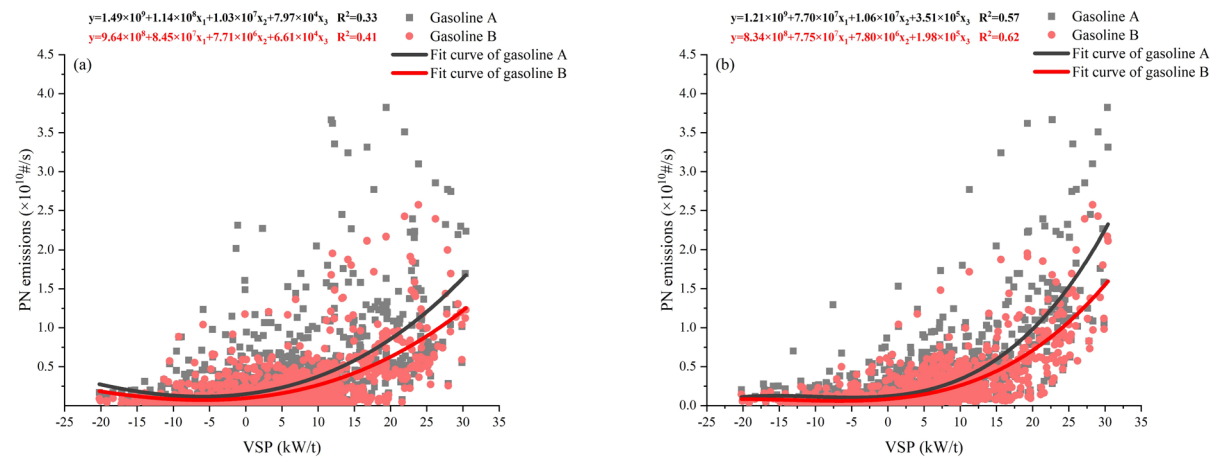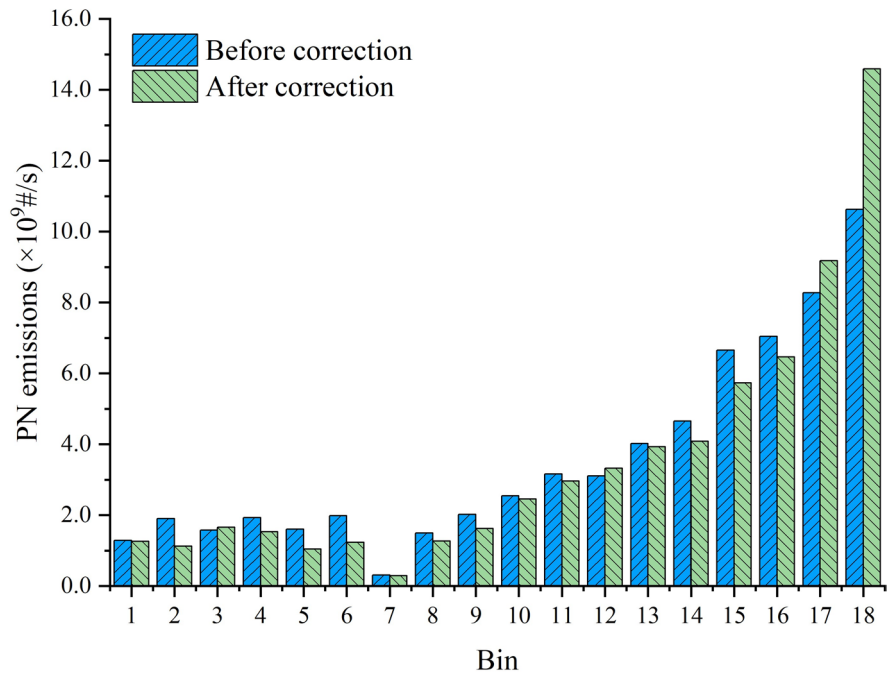**Fig. 6** Distribution of PN emissions rates in different bins of VSP: before and after correction

Fig. 7 Relationships of VSP and PN emissions (before correction (**a**) and after correction (**b**))

PN emissions after 10s was taken as the instantaneous PN concentration of the current working point, and the impacts of driving behavior on PN emissions were investigated.

As shown in Fig. S3, the effects of four driving states on emissions was analyzed, and the PN instantaneous emissions rate had been corrected. The average emission rate of PN was calculated for each of the four driving states. The results of

the four vehicles in different modes were shown in Fig. S3 a, b, c, and d. PN emissions were much higher in acceleration mode than in constant speed mode, with an average increase of $76\% \pm 34\%$. The reason was that the acceleration led to an increase in the concentration of fuel and air mixing in the combustion chamber, and incomplete combustion occurred(Banerjee & Christian, 2019; Gao et al., 2022). Compared to constant speed, PN emissions

in the deceleration state were reduced by $29\% \pm 8\%$. When decelerating, fuel consumption was reduced and pollutant emissions were reduced.

The distribution of PN instantaneous emissions with different driving speeds and acceleration of vehicle 1 was shown in Fig. 8, and the distribution of other vehicles is shown in Fig. S4 in the SI. The instantaneous PN emissions increased with the increase of vehicle speed and acceleration. Huang et al. reported that high acceleration and high speed conditions were acute events in PN emissions of vehicles (Huang et al., 2022). In this case, excessive fuel injection led to uneven mixing in the combustion chamber, resulting in high PN emissions(Wang et al., 2016). Furthermore, it could be seen from Fig. 8 that acceleration significantly affected PN emissions, especially when acceleration was 1.0–1.5 m/s², PN emissions increased significantly. However, when the acceleration was constant and the speed was less than 80 km/h, there was little difference in the PN emissions rate. Gao et al. reported a similar phenomenon, finding that the PN emissions were more sensitive to acceleration and the PN emissions tended to be high under high speed and acceleration conditions (Gao et al., 2022). In order to reduce emissions, drivers should reduce the occurrence of intense driving behavior on actual roads, especially at high speeds.

Conclusion

The gasoline with lower aromatic hydrocarbons and olefin content reduced PM and PN emissions by 24% and 52%, respectively. Due to the cold start, the average emission rate of PN during the first 300 s was 7.2 times that of the 300 s–1800s period during the WLTC test.

Due to the transmission time of particles in the test system and the response time of the instrument, there was some delay time between the true value and the measured value of PN instantaneous emissions. By comparing the Spearman correlation coefficient between PAVSP and the test results of PN instantaneous emission, the delay time was determined as 10s. Driving behavior had a strong impact on emissions. Acceleration increased PN emissions by 76% compared to the constant speed state. The increasing speed and acceleration led to the larger PN emissions and PN emissions were more sensitive to acceleration.

This study is helpful to establish the emission inventories of PN for China-VI gasoline vehicles, and contributes to control PN emissions. The delay phenomenon will lead to a large error in the measurement of the instantaneous emission rate of emission factors, which can affect fuel-based and power-based emission factors directly. Thus, this study helps to

Fig. 8 Distribution of PN instantaneous emissions with different driving speeds and acceleration of vehicle 1
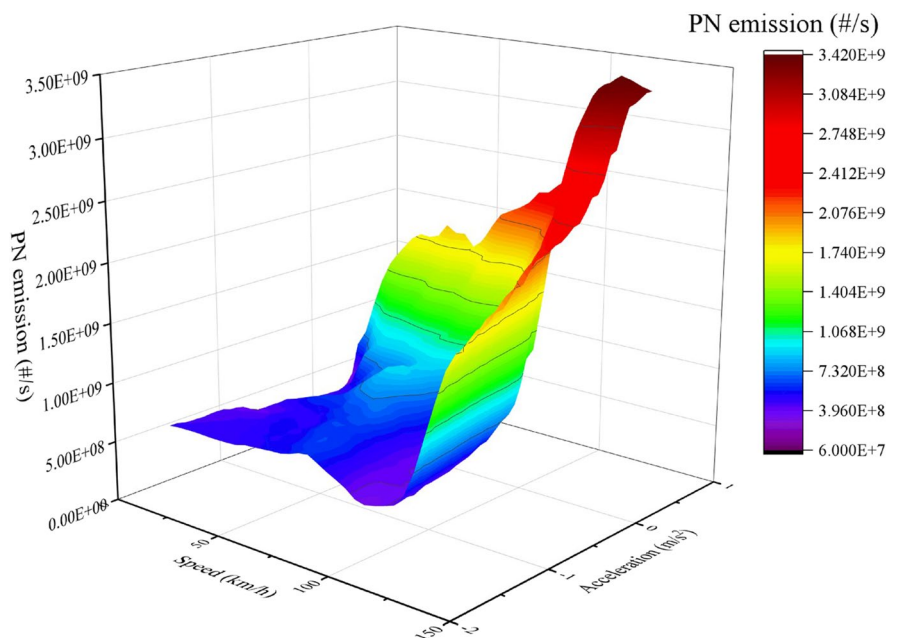
improve the accuracy of the analysis of emission factors. The disadvantage of this study is the small sample size, and the impact of gasoline on emissions is insufficient from the perspective of mechanism.

Authors' contributions   iaohan Miao (First Author): Conceptualization, Methodology, Software, Investigation, Formal Analysis, Writing - Original Draft; Xin Zhang:Data Curation, Writing - Original Draft; Chang Wang: Data Curation, Formal Analysis; Jingyuan Li (Corresponding Author):Resources, Supervision; Jie Zhao:Visualization, Investigation; Liang Qu:Visualization, Review; Yu Liu:Resources, Supervision; Songbo Qi:Review & Editing; Honglin Li:Review & Editing; Mengqi Fu:Investigation, Formal Analysis; Taosheng Jin (Corresponding Author):Conceptualization, Funding Acquisition, Resources, Supervision, Writing - Review & Editing.

Data availability   No datasets were generated or analyzed during the current study.

Declarations

Ethical approval   All authors have read, understood, and have complied as applicable with the statement on "Ethical responsibilities of Authors" as found in the Instructions for Authors and are aware that with minor exceptions, no changes can be made to authorship once the paper is submitted.

Competing interests   The authors declare no competing interests.

References

Abhishek, D., & Orathai, C. (2023). Assessment of health burden due to the emissions of fine particulate matter from motor vehicles: A case of Nakhon Ratchasima province, Thailand. *The Science of the Total Environment, 872*, 162128–162128. https://doi.org/10.1016/j.scitotenv.2023.162128

Alashaab, A., Saleh, H., Abo-Serie, E., & Rabee, B. (2016). Gaseous fuel for lower emissions during the cold start and warming up of spark ignition engines. *International Journal of Global Warming, 10*(1/2/3), 115–132. https://doi.org/10.1504/IJGW.2016.077909

An, F., Barth, M., Norbeck, J., & Ross, M. (1997). Development of comprehensive modal emissions model: Operating under hot-stabilized conditions. *Transportation Research Record, 1587*(1), 52–62. https://doi.org/10.3141/1587-07

Banerjee, T., & Christian, R. (2017). On-field and laboratory measurement of nanoparticle emission in the wake of gasoline vehicle. *Atmospheric Pollution Research, 8*(6), 1179–1192. https://doi.org/10.1016/j.apr.2017.05.007

Banerjee, T., & Christian, R. (2019). Effect of operating conditions and speed on nanoparticle emission from diesel and gasoline driven light duty vehicles. *Atmospheric Pollution Research, 10*(6), 1852–1865. https://doi.org/10.1016/j.apr.2019.07.017

Chen, L., Liang, Z., Zhang, X., & Shuai, S. (2017). Characterizing particulate matter emissions from GDI and PFI vehicles under transient and cold start conditions. *Fuel, 189*, 131–140. https://doi.org/10.1016/j.fuel.2016.10.055

Davis, N., Lents, J., Osses, M., Nikkila, N., & Barth, M. (2005). Development and application of an international vehicle emissions model. *Transportation Research Record, 1939*(1), 156–165. https://doi.org/10.1177/0361198105193900118

USEPA. (2009). *Technical guidance on the use of MOVES2010 for emission inventory preparation in state implementation plans and transportation conformity*. U.S. Environmental Protection Agency Retrieved March 30, 2024, from https://purl.fdlp.gov/GPO/LPS123823

Fang, G., Kao, C., Zhuang, Y., & Huang, P. (2021). Ambient air particulates and hg(p) concentrations and dry depositions estimations, distributions for various particles sizes ranges. *Journal of Environmental Science and Health, Part A, 56*(6), 1–8. https://doi.org/10.1080/10934529.2021.1918976

Frey, C., Rouphail, H., Zhai, M. N., Tiago, N., Farias, L., & Gonçalo, A. G. (2007). Comparing real-world fuel consumption for diesel- and hydrogen-fueled transit buses and implication for emissions. *Transportation Research Part D: Transport and Environment, 12*(4), 281–291. https://doi.org/10.1016/j.trd.2007.03.003

Gallus, J., Kirchner, U., Vogt, R., Christoph, B., & Thorsten, B. (2016). On-road particle number measurements using a portable emission measurement system (PEMS). *Atmospheric Environment, 124*, 37–45. https://doi.org/10.1016/j.atmosenv.2015.11.012

Gao, J., Wang, Y., Chen, H., Laurikko, J., Liu, Y., Pellikka, A. P., & Li, Y. (2022). Variations of significant contribution regions of NOx and PN emissions for passenger cars in the real-world driving. *Journal of Hazardous Materials, 424*(PC), 127590. https://doi.org/10.1016/J.JHAZMAT.2021.127590

Giechaskiel, B., Lähde, T., & Drossinos, Y. (2019). Regulating particle number measurements from the tailpipe of light-duty vehicles: The next step? *Environmental Research, 172*, 1–9. https://doi.org/10.1016/j.envres.2019.02.006

Hannelore, B., Eva, B., Eli, S., Bijnens, E., et al. (2019). Ambient black carbon particles reach the fetal side of human placenta. *Nature Communications, 10*(1), 3866. https://doi.org/10.1038/s41467-019-11654-3

Huang, J., Gao, J., Wang, Y., Yang, C., & Chaochen, M. (2022). Real-world pipe-out emissions from gasoline direct injection passenger cars. *Processes, 11*(1), 66. https://doi.org/10.3390/PR11010066

Ioannis, M., Elisavet, S., Agathangelos, S., & Eugenia, B. (2020). Environmental and health impacts of air pollution:

A review. *Frontiers in Public Health, 8*, 14. https://doi.org/10.3389/fpubh.2020.00014

Jiménez, P. J. L. (1999). *Understanding and quantifying motor vehicle emissions with vehicle specific power and TILDAS remote sensing*. Thesis (Ph.D.), Massachusetts Institute of Technology, Dept. of Mechanical Engineering, Massachusetts Institute of Technology.

Karavalakis, G., Daniel, S., Diep, V., Robert, R., Maryam, H., Akua, A., & A., & Thomas, D. D. (2015). Evaluating the effects of aromatics content in gasoline on gaseous and particulate matter Emissions from SI-PFI and SIDI vehicles. *Environmental Science & Technology, 49*(11), 7021–7031. https://doi.org/10.1021/es5061726

Ko, J., Kim, K., Chung, W., Myung, C., & Park, S. (2019). Characteristics of on-road particle number (PN) emissions from a GDI vehicle depending on a catalytic stripper (CS) and a metal-foam gasoline particulate filter (GPF). *Fuel, 238*, 363–374. https://doi.org/10.1016/j.fuel.2018.10.091

Lents, J., & Davis, N. (2004). *IVE model users manual*. ISSRC.

Li, G., Zeng, Q., & Pan, X. (2016). Disease burden of ischaemic heart disease from short-term outdoor air pollution exposure in Tianjin, 2002–2006. *European Journal of Preventive Cardiology, 23*(16), 1774–1782. https://doi.org/10.1177/2047487316651352

Liu, F., Zhao, F., Liu, Z., & Hao, H. (2020). The impact of purchase restriction policy on Car ownership in China's four major cities. *Journal of Advanced Transportation, 2020*, 1–14. https://doi.org/10.1155/2020/7454307

Liu, H., & Barth, M. (2012). Identifying the effect of vehicle operating history on vehicle running emissions. *Atmospheric Environment, 59*, 22–29. https://doi.org/10.1016/j.atmosenv.2012.05.045

Liu, J., Ge, Y., Wang, X., Hao, L., Tan, J., Peng, Z., Zhang, C., Gong, H., & Huang, Y. (2017). On-board measurement of particle numbers and their size distribution from a light-duty diesel vehicle: Influences of VSP and altitude. *Journal of Environmental Sciences, 57*, 238–248. https://doi.org/10.1016/j.jes.2016.11.023

Ministry of Ecology and Environment of the People's Republic of China (MEE). (2016). Limits and measurement methods for emissions from light-duty vehicles (CHINA 6), : China Environment Press. Retrieved May 28, 2024, from https://www.mee.gov.cn/gkml/hbb/bgg/201612/t20161223_369497.htm

Ministry of Ecology and Environment of the People's Republic of China (MEE). (2022). China Vehicle Environmental Management Annual Report. Retrieved July 9, 2023, from https://www.mee.gov.cn/hjzl/sthjzk/ydyhjgl/202212/t20221207_1007111.shtml

Pan, M., Huang, R., Liao, J., Jia, C., Zhou, X., Huang, H., & Huang, X. (2019). Experimental study of the spray, combustion, and emission performance of a diesel engine with high n -pentanol blending ratios. *Energy Conversion and Management, 194*, 1–10. https://doi.org/10.1016/j.enconman.2019.04.054

Sandhu, S. G., & Frey, C. H. (2013). Effects of errors on vehicle emission rates from portable emissions measurement systems. *Transportation Research Record: Journal of the Transportation Research Board, 2340*(1), 10–19. https://doi.org/10.3141/2340-02

Tang, G., Wang, S., Du, B., Cui, L., Huang, Y., & Xiao, W. (2022). Study on pollutant emission characteristics of different types of diesel vehicles during actual road cold start. *Science of the Total Environment, 823*, 153598. https://doi.org/10.1016/J.SCITOTENV.2022.153598

Wang, Y., Zheng, R., Qin, Y., Peng, J., Li, M., Lei, J., Wu, Y., Hu, M., & Shuai, S. (2016). The impact of fuel compositions on the particulate emissions of direct injection gasoline engine. *Fuel, 166*, 543–552. https://doi.org/10.1016/j.fuel.2015.11.019

Wei, J., Zenghui, Y., Yejian, Q., Chenfang, W., & Chen, B. (2019). Comparative effects of olefin content on the performance and emissions of a modern GDI engine. *Energy & Fuels, 33*(11), 10499–11050. https://doi.org/10.1021/acs.energyfuels.9b01894

World Health Organization. (2021). WHO global air quality guidelines: Particulate matter (PM2.5 and PM10), ozone, nitrogen dioxide, sulfur dioxide and carbon monoxide. Retrieved July 29, 2023, from https://www.who.int/publications/i/item/9789240034228.

Wu, R., Zhong, L., Huang, X., Xu, H., Liu, S., Feng, B., Wang, T., Song, X., Bai, Y., Wu, F., Wang, X., & Huang, W. (2018). Temporal variations in ambient particulate matter reduction associated short-term mortality risks in Guangzhou, China: A time-series analysis (2006–2016). *Science of the Total Environment, 645*, 491–498. https://doi.org/10.1016/j.scitotenv.2018.07.091

Xu, J., Tu, R., Wang, A., Zhai, Z., & Hatzopoulou, M. (2020). Generation of spikes in ultrafine particle emissions from a gasoline direct injection vehicle during on-road emission tests. *Environmental Pollution, 267*(prepublish), 115695. https://doi.org/10.1016/j.envpol.2020.115695

Yang, D., Hua, Z., Wang, Z., Zhao, S., & Li, J. (2021). Changes in anthropogenic particulate matters and resulting global climate effects since the industrial revolution. *International Journal of Climatology, 1*, 315–330. https://doi.org/10.1002/JOC.7245

Yang, J., Roth, P., Zhu, H., Thomas, D. D., & Karavalakis, G. (2019). Impacts of gasoline aromatic and ethanol levels on the emissions from GDI vehicles: Part 2. Influence on particulate matter, black carbon, and nanoparticle emissions. *Fuel, 252*, 812–820. https://doi.org/10.1016/j.fuel.2019.04.144

Zhang, X., Zhang, L., Li, J., Zou, X., Jing, X., & Li, W. (2022). Combustion and emission characteristics of diesel with different distillation ranges on the China-VI diesel engine.

Fuel, 325, 124876. https://doi.org/10.1016/J.FUEL.2022.124876

Zhao, H., Jing, D., Wang, Y., Shuai, S., & Pang, C. (2017). *Effects of aromatic and olefin on the formations of PAHs in GDI engine* (p. 2390). SAE Technical Paper Series. https://doi.org/10.1016/j.fuel.2021.120131

Zhou, H., Zhao, H., Wu, M., Li, J., Wang, J., Feng, Q., Long, Z., Yu, S., Peng, H., Wang, X., & Jin, T. (2019). Influence of different bin-grouping methods on the estimation of emission factors in model IVE in Chinese. *China Environmental Science, 39*(02), 560–564. https://doi.org/10.19674/j.cnki.issn1000-6923.2019.0067